



Long range emission enhancement and anisotropy in coupled quantum dots induced by aligned gold nanoantenna

L. N. Tripathi, M. Praveena, Pranay Valson, and J. K. Basu

Citation: [Applied Physics Letters](#) **105**, 163106 (2014); doi: 10.1063/1.4900521

View online: <http://dx.doi.org/10.1063/1.4900521>

View Table of Contents: <http://scitation.aip.org/content/aip/journal/apl/105/16?ver=pdfcov>

Published by the [AIP Publishing](#)

Articles you may be interested in

[Highly polarized light emission by isotropic quantum dots integrated with magnetically aligned segmented nanowires](#)

Appl. Phys. Lett. **105**, 141116 (2014); 10.1063/1.4897971

[Three-dimensional photoluminescence mapping and emission anisotropy of single gold nanorods](#)

Appl. Phys. Lett. **100**, 263102 (2012); 10.1063/1.4729152

[Enhanced spontaneous emission from quantum dots in short photonic crystal waveguides](#)

Appl. Phys. Lett. **100**, 061122 (2012); 10.1063/1.3683541

[Tuning of Long range Visible Emissions Using Coupled Quantum Dots](#)

AIP Conf. Proc. **1349**, 277 (2011); 10.1063/1.3605842

[Anisotropic and enhanced absorptive nonlinearities in a macroscopic film induced by aligned gold nanorods](#)

Appl. Phys. Lett. **96**, 263103 (2010); 10.1063/1.3458693

Over **600** Multiphysics Simulation Projects

[VIEW NOW >>](#)

COMSOL

The advertisement features a 3D simulation of a red cylindrical component with a silver-colored internal structure. A rainbow-colored light beam is shown passing through the structure. The background is dark with a grid pattern. The text 'Over 600 Multiphysics Simulation Projects' is prominently displayed in white and blue. A blue button with white text 'VIEW NOW >>' is located on the right. The COMSOL logo is in the bottom right corner.

Long range emission enhancement and anisotropy in coupled quantum dots induced by aligned gold nanoantenna

L. N. Tripathi,^{a)} M. Praveena, Pranay Valson,^{b)} and J. K. Basu^{c)}

Department of Physics, Indian Institute of Science, Bangalore 560012, India

(Received 6 June 2014; accepted 13 October 2014; published online 23 October 2014)

Quantum dot arrays have been projected as the material of choice for next generation displays and photodetectors. Extensive ongoing research aims at improving optical and electrical efficiencies of such devices. We report experimental results on non-local long range emission intensity enhancement and anisotropy in quantum dot assemblies induced by isolated and partially aligned gold nanoantennas. Spatially resolved photoluminescence clearly demonstrate that the effect is maximum, when the longitudinal surface plasmon resonance of the nanoantenna is resonant with the emission maxima of the quantum dots. We estimated the decay length of this enhancement to be $\sim 2.6 \mu\text{m}$, which is considerably larger than the range of near field interaction of metal nanoantenna. Numerical simulations qualitatively capture the near field behavior of the nanorods but fail to match the experimentally observed non-local effects. We have suggested how strong interactions of quantum dots in the close packed assemblies, mediated by the nanoantennas, could lead to such observed behavior. © 2014 AIP Publishing LLC. [<http://dx.doi.org/10.1063/1.4900521>]

An assembly of quantum dots is an ideal system in which coupling between individual dots through their charge, spin, or optical excitation can be studied.^{1–4} Apart from these fundamental aspects of Physics such systematic studies will have important implications in a wide range of fields from photovoltaic to displays and quantum information processing.^{5–7} This has motivated research^{8–10} aiming at exploring the possibilities of coupling excitons for improved efficiency in photovoltaic and photonic devices. One of the ways to improve optical coupling in quantum emitters is to use plasmonic nanoantenna.^{5,11} There has been an enormous surge in research on plasmonic nanoantenna in last few years especially in trying to understand the efficiency of their coupling with optical emitter.^{5,12,13} Various types of nanoantennas have been fabricated using different methods.^{4,14,15} The simplest of these is the elongated single or multiple metal nanorod or nanowires system with well defined radiative properties.^{16–19} We have shown earlier²⁰ that for small concentrations of the simplest plasmonic nanoantenna—spherical gold nanoparticles—unexpected enhancement in photoluminescence (PL) can be obtained in compact and coupled cadmium selenide (CdSe) quantum dot assemblies, mediated essentially by plasmonic Dicke effect.²¹ How does the doping with low concentration of gold nanorods (GNR) nanoantenna modify the emission from compact quantum dot assemblies? What are the regimes of PL intensity enhancement and quenching? Is there polarisation dependence induced in the quantum dot emission due to the anisotropic structure of the GNR nanoantenna? In case there is enhancement, as was observed earlier by us²⁰ for spherical nanoantenna, is the

spatial extent of this enhancement near field only or is it long range, due to possible excitation of some collective modes in the close packed quantum dot assemblies?

To address some of these questions, we have performed experiments on studying polarisation dependent PL measurements on coupled spherical monolayer quantum dot assemblies onto which randomly dispersed, but partially aligned GNR antenna were incorporated. We observed non-local anisotropy and enhancement of PL in quantum dots induced by the GNR nanoantenna located at distance significantly larger than the decay length of the near field due to longitudinal surface plasmon resonance (LSPR) of the rods. Such long range interaction is most efficient when the quantum dot PL emission wavelength is resonant with the LSPR of the GNR nanoantenna. Numerical simulations qualitatively capture the near field behavior of the nanorods but fail to match the experimentally observed non-local effects. We have indicated, qualitatively, how strong interactions of quantum dots in the close packed assemblies, mediated by the GNR nanoantennas, could lead to such observed behavior. Our results indicate the possibility of utilizing this non-local effect mediated by cooperative interactions between plasmons and excitons in such hybrid assemblies to enhance nanoscale energy transfer for potential applications in wide range of areas from light emitting devices and photodetectors to photovoltaics.

To study the coupling between quantum dots and GNR nanoantenna, large scale compact assemblies of colloidal Cadmium selenide (CdSe) quantum dots (Q) with a core diameter of 10 nm were prepared on glass substrates by the Langmuir-Blodgett (LB) method, as described earlier.^{20,22} Gold nanorods of aspect ratio (AR) 2 (A1) and 3 (A2) were transferred onto LB prepared quantum dot assemblies, described above, using dip coating method from their respective solutions in water. Typical transmission electron microscopy (TEM) images of such a film showing one GNR with the quantum dot monolayer background is shown in

^{a)}Present address: Center for Subwavelength Optics, Department of Physics and Astronomy, Seoul National University, 1 Gwanak-ro, Gwanak-gu, Seoul 151-747, South Korea.

^{b)}Present address: FUSION-EP, Erasmus Mundus, Institute of Interfacial Process Engineering and Plasma Technology (IGVP), Universitt Stuttgart, Germany.

^{c)}basu@physics.iisc.ernet.in

Figs. 1(a) and S5 (Ref. 23). From the UV visible and PL spectroscopy data on the solutions of the GNRs and quantum dots, presented in Fig. S6 (Ref. 23), it is clear that while A1 GNRs have their LSPR peaks resonant with the PL emission peak of quantum dots while that of A2 GNRs is considerably red shifted and hence off-resonant with the quantum dot emission. We now discuss the emission properties of the films of these three samples, Q, A1, and A2, under **p** and **s** excitation in confocal mode collected using the setup shown in Figs. 1(b) and 1(c) with 633 nm incident radiation. All PL spectra were collected at constant incident laser intensity and several such spectra were collected at different regions of the respective samples. Figure 2 shows typical spatial light intensity map of effective enhancements of PL from A1 films relative to Q film. Here, $F = \frac{I_{hyb}}{I_{qd}}$, where I_{hyb} and I_{qd} are PL intensity from the hybrid and quantum dot monolayer, respectively. We observe strong spatial inhomogeneity for A1 films, while for A2 films this is negligible and comparable to that of Q films. Further, we quantified the PL spectral anisotropy G_{PL} , $G_{PL} = \left| \frac{I_p - I_s}{I_p + I_s} \right|$, where I_p and I_s are PL intensity under **p** and **s** excitation, respectively. The spatial map of G_{PL} , from confocal microscopy, for A1 and A2 films is shown in Figs. 2(c) and 2(d), respectively. Remarkably, sample A1 shows typical maximum anisotropy of 0.66 and even the minimum value recorded was 0.45 within the scan range (see Table I). In contrast, typical G_{PL} for A2 sample is ~ 0.10 at the most and hence comparable to the values observed for the Q films (Fig. S14 (Ref. 23)) which in some sense provides an estimate of the sensitivity of these measurements. To correlate the spatial variation of F and G_{PL} with morphology better, we have also performed even higher

spatial resolution PL spectroscopy on these samples using near-field scanning microscopy (NSOM).

Figure 2(e) shows a typical NSOM topography image from sample A1. Typical separation between various GNR assemblies as can be seen from this (and Fig. S10 (Ref. 23)) is $(0.5\text{--}2.0)\ \mu\text{m}$. In Fig. 2(f), we also summarize the spatial variation of F under **p** excitation for a typical region of the sample A1, showing GNR assemblies, in the background of the compact quantum dot monolayer. Both F and G_{PL} [supplementary material, Fig. S14(c)] show maxima near GNR assemblies which decay away from these regions. This is similar to earlier observations.^{24,25} However, what is striking is that $F \gg 1$ and $G_{PL} \gg 0$ at locations far away from any GNR assemblies (see Table I). This is indicative of some form of non-local and long range coupling between GNR mediated by the quantum dots in the compact quantum dot monolayer. The maximum in F and G_{PL} occur in plasmonic *hot spots* (between regions marked 2, 3, and 4 in Fig. 2(e)). In Fig. 2(h), we present the corresponding PL intensity enhancement and anisotropy maps (Fig. 2(d)) for A2 sample. The typical separation between the GNRs in this case is $(0.3\text{--}5.0)\ \mu\text{m}$ (Fig. 2(g)). Interestingly, we see negligible PL enhancement as well as anisotropy for these films for identical density of quantum dots as for A1 films. The maximum (G_{PL}) measured for this sample is 0.06 (Fig. S14(d)), which is considerably smaller than even the minimum observed values in A1. The maximum enhancement $F \sim 1$ and again considerably smaller than that observed for A1 sample especially for **p**—polarization (Fig. 2(a)). Moreover, the observed variations in G_{PL} (Fig. S14(d)) is uncorrelated to the corresponding topographical features in Fig. 2(g).

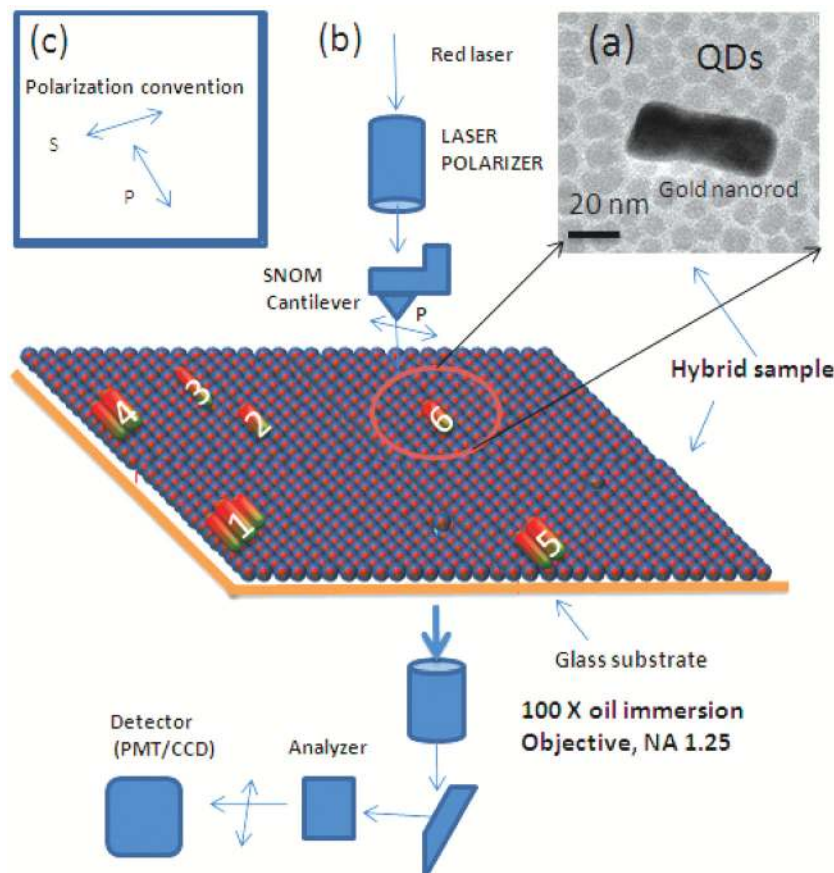


FIG. 1. Experimental set up: (a) TEM image showing a typical GNR over the CdSe quantum dots monolayer. (b) Schematic diagram for sample details and NSOM setup where incident polarized beam is raster scanned over a gold nanorods sitting over a monolayer of quantum dots. (c) **p** and **s** refers to incident polarization of laser beam parallel and perpendicular to length of gold nanorods.

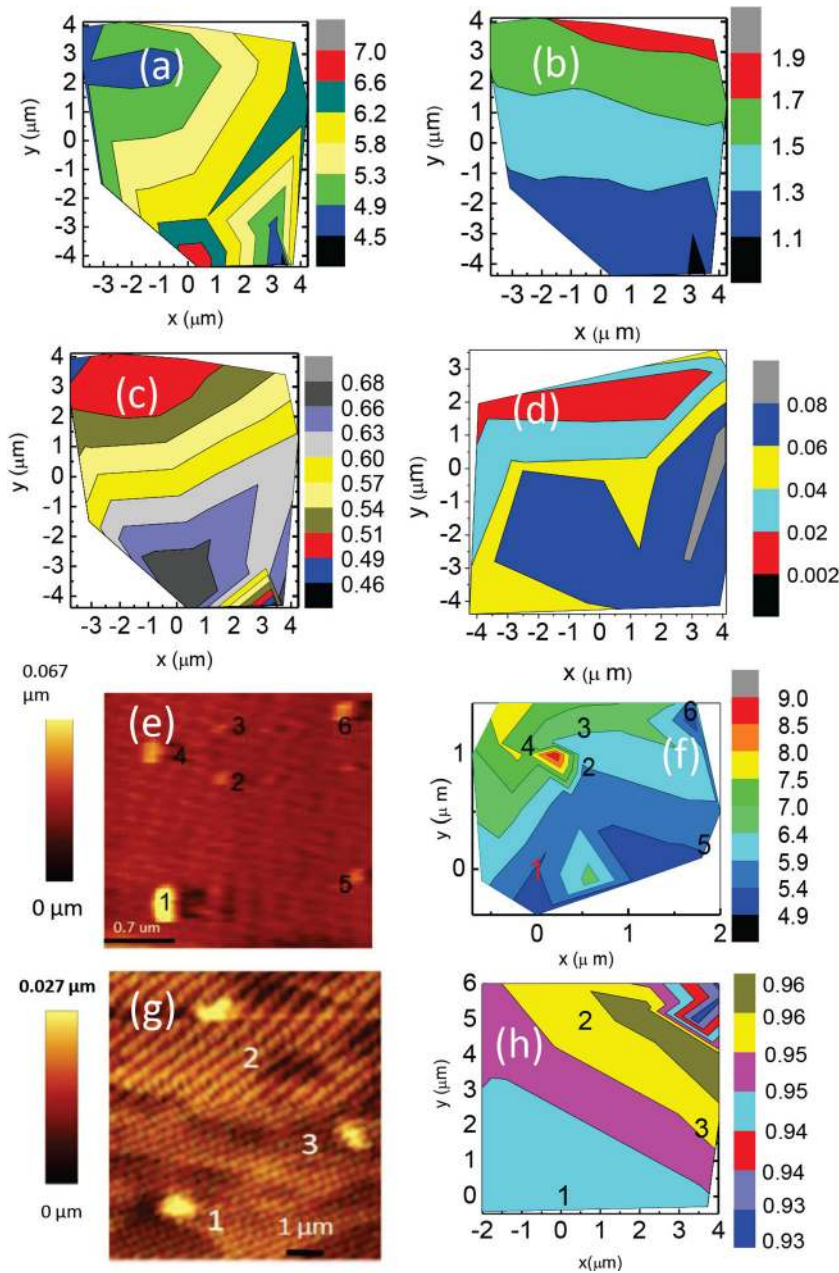


FIG. 2. Confocal PL enhancement maps for (a) A1 under \mathbf{p} excitation and for (b) A2 under \mathbf{s} excitation. Confocal PL anisotropy map for (c) A1 film and (d) A2 film. NSOM topography image for (e) A1 and for (g) A2. PL enhancement factor from (f) A1 and (h) A2 both under \mathbf{p} excitation.

Another convincing proof of the authenticity of the results also lies in the fact that $F \sim 1$ and $G_{PL} \sim 0$ for sample A2 for which the GNR LSPR is red shifted significantly from the quantum dot PL emission (Fig. S6(b) (Ref. 23)) maxima and the excitation wavelength and is hence off-resonant. This observation also strongly suggests the presence of nanoantenna

TABLE I. PL spectral parameters for various samples: F , enhancement in PL from hybrid with respect to the quantum dot monolayer, G_{PL} being anisotropy in PL, respectively, and P is polarization of incident laser.

Sample	P	G_{PL}	F
Q	\mathbf{p}	0.014	
A1	\mathbf{p}	0.30–0.60	5.00–9.00
A2	\mathbf{p}	0.02–0.06	0.48–0.98
Q	\mathbf{s}		
A1	\mathbf{s}		1.60–3.30
A2	\mathbf{s}		0.78–0.98

effect produced by GNRs at resonance. Thus, the confocal and NSOM PL spatial map results are very similar although due to the finer spatial resolution in NSOM mode, the correlation of GNR assembly morphology to the observed value of F and G_{PL} can be clearly made, unlike that in confocal mode.

To quantify, further, the process of this long range enhancement, especially to provide the estimate of range and the functional form of its distance dependence, we have performed measurements of PL intensity, with \mathbf{p} polarized 633 nm light, spanning the interface between regions on quantum dot films with and without GNRs for A1 samples, which showed clear PL enhancement. Figure 3 shows typical confocal PL intensity image in the region of A1 film without GNRs (Fig. 3(a)) and also the interface region (Fig. 3(b)). While the intensity is fairly homogeneous in the region of A1 film without GNRs (lines D and E), the interface region shows clear intensity gradient from GNR populated region to the bare quantum dot region (line C), perpendicular to the

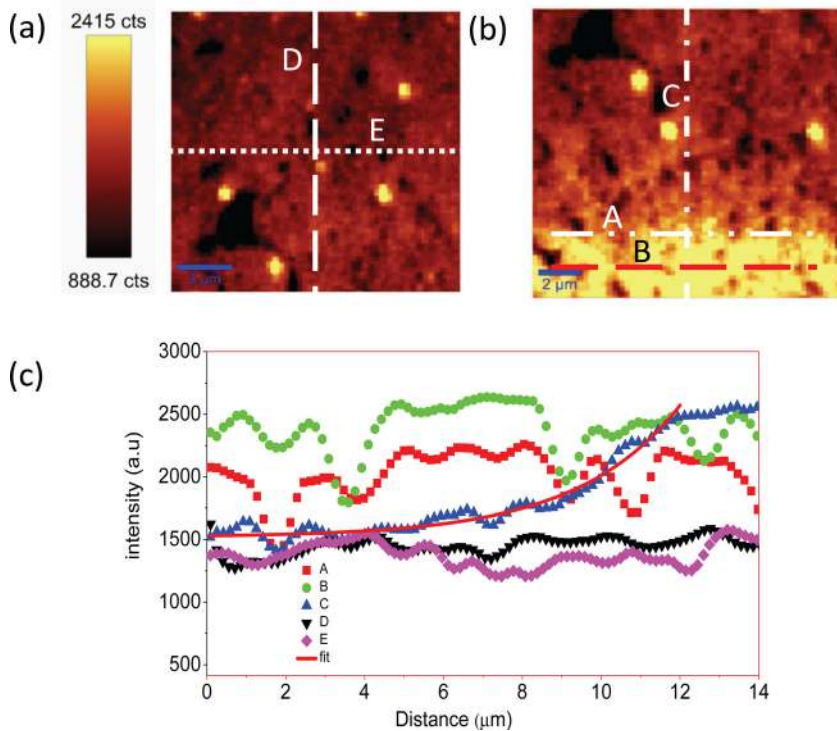


FIG. 3. (a) Light intensity image of Al film of regions without GNRs and (b) interface of quantum dots and GNRs. Here, the light intensity scale bar shown in (a) is common to both (a) and (b). (c) PL intensity distributions along the lines drawn and as indicated by lines shown in panels (a) and (b). The gradient along the interface (blue line) can be clearly distinguished from the flat line profiles with random fluctuations due to breakages in film. The solid line (red) indicates the fit to the gradient profile with an exponential function.

interface. On the contrary, the PL intensity line profiles along the interface (lines marked A and B in Fig. 3(b)) show fluctuations due to defects in the quantum dot film and variation in GNR density but show no discernible gradients. This suggests that GNR density gradients are not responsible for the observed PL enhancement profiles. We have also extracted several line profiles across such regions, one of which (a typical one) is shown in Fig. 3(c). The PL intensity decay profile across the interface, in Fig. 3(c), fits very nicely with an exponential distance dependent function (Table SII and Eq. (1) of supplementary material).²³ From the line profiles, we have extracted the decay length of the spatial extent of PL enhancement, due to the partially aligned GNRs as $2.6 \pm 0.1 \mu\text{m}$. This is a significantly larger spatial range of energy transfer compared to the expected near field range for GNRs, as will become clear later. In addition, the range is also much larger than the range estimated for coupling between large quantum dots leading to super-radiance behavior.²

To obtain possible insight into the mechanism underlying the observed non local PL enhancement and anisotropy finite difference time domain (FDTD) simulations,²³ an effective scheme, for such hybrid systems have been performed. Figure 4 shows snapshots of the electric field profile near a typical GNR (AR 2 and AR 3)-quantum dot monolayer interface, when excited with 633 nm radiation. The corresponding near field spatial profiles are also shown in Fig. 4(c) and indicate, expected, large resonant field enhancement for AR 2 GNRs compared to AR 3, but the field enhancement is limited to a distance of ~ 50 nm from the GNR surface. The field strength for the *s* is smaller than that in *p*. Thus, although the qualitative trends of our experimentally observed PL enhancement and the emission anisotropy in the near field of the GNR nanoantenna are similar to the predicted electric field enhancement and emission anisotropy from FDTD, the far field effects do not match. Since FDTD fails to capture the observed long range energy transfer, we

propose a qualitative model to help understand our observations, especially with respect to the NSOM mode illumination.

Let us imagine that the NSOM probe illuminates a small region of compact quantum dots far away from any GNR as

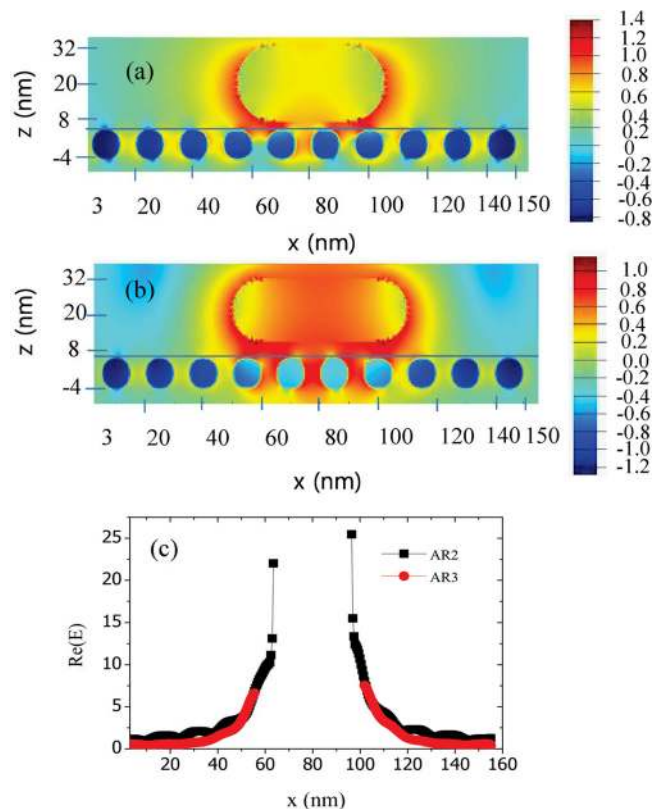


FIG. 4. Absolute electric field intensity color map at all points along longitudinal cross section of hybrid plane for (a) A1 (diameter 25 nm; length 50 nm), (b) A2 (diameter 20 nm; Length 60 nm). (c) Absolute electric field intensity decay profile for (a) and (b) (for the lines drawn in color map).

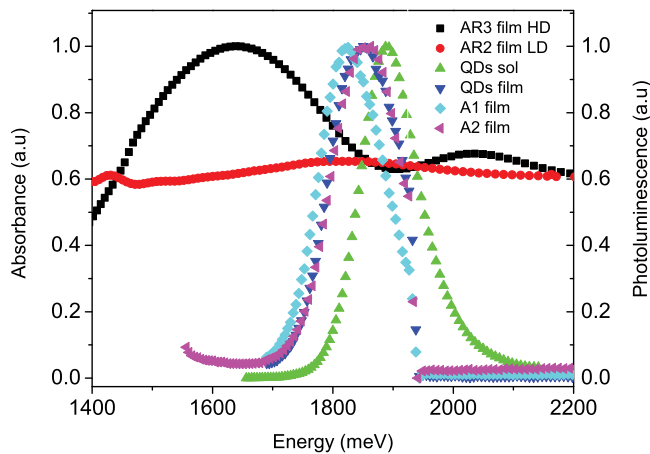


FIG. 5. Absorbance spectra from compact film of gold nanorod of aspect ratio 2 (AR2) and 3 (AR3) transferred over glass. Normalized NSOM PL spectra from the quantum dots in toluene (QDs sol) and quantum dot film (QDs film), A1 film and A2 film. Here, the AR2 film low density (LD) is scaled up by a factor of 337 times and that of AR3 film high density (HD) by a factor of 2 for better visibility.

shown in the Video (Ref. 23). If there were only one or few quantum dots in this illuminated area, the PL emission from them would decay significantly before it reaches near GNR and hence cannot feel the nanoantenna induced radiative enhancements. However, with the close packed layer, the PL emission is effectively transferred to the nearby GNR assembly through the neighboring quantum dots. Since, the total time integrated (~ 199 ms) PL spectra is collected in far field geometry and includes the significant enhanced PL emission coming from the region with GNR assemblies as well, the total measured PL intensity is enhanced, even for initial excitation in regions having no GNRs. Evidence for energy transfer between close packed quantum dots can be seen (Fig. 5) from the fact that there is red shift of 83 meV in PL from Q film compared to quantum dot solution PL as observed earlier¹ while that between the GNR and quantum dots is evidenced from a further shift in PL spectral maxima of 28 meV from A1 film with respect to quantum dot film. This additional shift is almost absent in A2 film as seen in Fig. 5. Since the excited nanoantenna mode is itself polarized the observed PL emission from the quantum dots, is also polarized. The fact that excitation of the nanoantenna mode is important can be seen from the fact that the non-resonant GNR can neither be excited by the laser line 633 nm nor by the quantum dot PL emission and hence does not show any change in F and G .

In conclusion, we have demonstrated non-local far field enhancement of PL in quantum dots induced by isolated and partially aligned GNR nanoantenna located on such assemblies. The emission is also anisotropic with the maxima being near such GNR assembly which decays to finite, non-zero, and significantly large values, even away from the vicinity of any such assemblies. The decay length of such PL intensity enhancement was found to be $\sim 2.6 \pm 0.1 \mu\text{m}$. Although the FDTD simulations can model some of the

observed near field effects, the non-local long range effects cannot be effectively captured in such simulations. We have indicated, qualitatively, how strong interactions between quantum dots in the close packed assemblies, mediated by the GNR nanoantennas, could lead to such observed behavior. This, in turn, suggests the possibility of utilizing such non-local effects in metal-semiconductor hybrid assemblies to enhance nanoscale energy transfer for potential applications in various phenomena including, but not limited to, improved displays, photodetectors, light harvesting, and photovoltaics.

We acknowledge Department of Science and Technology (Nanomission), India, for financial support and Advanced Facility for Microscopy and Microanalysis, Indian Institute of Science, Bangalore, for access to TEM measurements. M. Praveena acknowledges UGC, India, for financial support.

- ¹C. R. Kagan, C. B. Murray, and M. G. Bawendi, *Phys. Rev. B* **54**, 8633 (1996).
- ²M. Scheibner, T. Schmidt, L. Worschech, A. Forchel, G. Bacher, T. Passow, and D. Hommel, *Nat. Phys.* **3**, 106 (2007).
- ³P. Chen, C. Piemarocchi, and L. Sham, *Phys. Rev. Lett.* **87**, 067401 (2001).
- ⁴A. G. Curto, G. Volpe, T. H. Taminiau, M. P. Kreuzer, R. Quidant, and N. F. van Hulst, *Science* **329**, 930 (2010).
- ⁵L. Novotny and N. van Hulst, *Nat. Photonics* **5**, 83 (2011).
- ⁶X. Wang, G. I. Koleilat, J. Tang, H. Liu, I. J. Kramer, R. Debnath, L. Brzozowski, D. A. R. Barkhouse, L. Levina, S. Hoogland *et al.*, *Nat. Photonics* **5**, 480 (2011).
- ⁷M. Ouyang and D. D. Awschalom, *Science* **301**, 1074 (2003).
- ⁸V. Klimov, A. Mikhailovsky, S. Xu, A. Malko, J. Hollingsworth, C. Leatherdale, H.-J. Eisler, and M. Bawendi, *Science* **290**, 314 (2000).
- ⁹H. A. Atwater and A. Polman, *Nat. Mater.* **9**, 205 (2010).
- ¹⁰K. S. Jeong, J. Tang, H. Liu, J. Kim, A. W. Schaefer, K. Kemp, L. Levina, X. Wang, S. Hoogland, R. Debnath *et al.*, *ACS Nano* **6**, 89 (2012).
- ¹¹V. Giannini, A. I. Fernandez-Domanguez, S. C. Heck, and S. A. Maier, *Chem. Rev.* **111**, 3888 (2011).
- ¹²E. S. Barnard, R. A. Pala, and M. L. Brongersma, *Nat. Nanotechnol.* **6**, 588 (2011).
- ¹³D. E. Chang, A. S. Sørensen, P. R. Hemmer, and M. D. Lukin, *Phys. Rev. Lett.* **97**, 053002 (2006).
- ¹⁴A. Kinkhabwala, Z. Yu, S. Fan, Y. Avlasevich, K. Müllen, and W. Moerner, *Nat. Photonics* **3**, 654 (2009).
- ¹⁵I. S. Maksymov and Y. S. Kivshar, *Opt. Lett.* **38**, 4853 (2013).
- ¹⁶A. V. Akimov, A. Mukherjee, C. L. Yu, D. E. Chang, A. S. Zibrov, P. R. Hemmer, H. Park, and M. D. Lukin, *Nature* **450**, 402 (2007).
- ¹⁷K. J. Russell, T.-L. Liu, S. Cui, and E. L. Hu, *Nat. Photonics* **6**, 459 (2012).
- ¹⁸P. Biagioni, J.-S. Huang, and B. Hecht, *Rep. Prog. Phys.* **75**, 024402 (2012).
- ¹⁹J. Dorfmueller, R. Vogelgesang, R. T. Weitz, C. Rockstuhl, C. Etrich, T. Pertsch, F. Lederer, and K. Kern, *Nano Lett.* **9**, 2372 (2009).
- ²⁰L. N. Tripathi, M. Praveena, and J. K. Basu, *Plasmonics* **8**, 657 (2013).
- ²¹V. Pustovit and T. Shahbazyan, *Phys. Rev. Lett.* **102**, 77401 (2009).
- ²²M. Haridas, L. N. Tripathi, and J. K. Basu, *Appl. Phys. Lett.* **98**, 063305 (2011).
- ²³See supplementary material at <http://dx.doi.org/10.1063/1.4900521> for details of synthesis and characterization of the GNR-QD hybrid assemblies, NSOM and confocal PL measurement, and finite difference time domain simulations.
- ²⁴S. Kawata, Y. Inouye, and P. Verma, *Nat. Photonics* **3**, 388 (2009).
- ²⁵T. Ming, H. Chen, R. Jiang, Q. Li, and J. Wang, *J. Phys. Chem. Lett.* **3**, 191 (2012).